Talanta 85 (2011) 2135–2141

Contents lists available at ScienceDirect

Talanta

journal homepage: www.elsevier.com/locate/talanta

Enzyme digestion of entrapped single-DNA molecules in nanopores

Seungah Lee[a], Seong Ho Kang[b,*], Edward S. Yeung[a,**]

[a] Ames Laboratory – USDOE, Department of Chemistry, Iowa State University, Ames, IA 50011, USA
[b] Department of Applied Chemistry, College of Applied Science, Kyung Hee University, Yongin-si, Gyeonggi-do 446-701, South Korea

ARTICLE INFO

Article history:
Received 1 June 2011
Received in revised form 12 July 2011
Accepted 15 July 2011
Available online 23 July 2011

Keywords:
Single-molecule
DNA
Enzyme digestion
Nanopore
3D environment

ABSTRACT

The real-time digestion of entrapped single-DNA molecules by λ-exonuclease in nanoporous alumina membranes was observed using an epifluorescence microscope. The alumina membrane provides pL ($\sim 10^{-12}$ L) containers for confining single-DNA molecules without immobilization. When one end of the DNA molecule was inserted into a nanopore, it was possible to monitor the digestion process outside, near and inside the pore, where the individual DNA molecules exhibited different characteristic digestion modes. The digestion rates calculated from the decrease in fluorescence intensity showed different values according to the location of the individual molecules. Entrapment rather than immobilization allows the DNA strand to be fully exposed to the enzyme and the reaction buffer. These results confirm that the enzymatic digestion of DNA molecules is affected by their three-dimensional (3D) environment.

1. Introduction

Ultra-sensitive detection and real-time observation are among the most important techniques for examining the behaviors of individual molecules, such as their conformational changes, dynamics or reactivity. Such studies allow much more detailed information to be gained than by performing ensemble-averaged measurements. Many biological applications of single-molecule detection (SMD) have been demonstrated [1–12]. In particular, in studies of enzyme activity, single-molecule measurements have been invaluable because the various conformers do not interconvert very quickly [13–20]. It was also demonstrated at single-molecule level that highly purified enzyme molecules have been shown to have identical activity [21].

Enzyme molecules have been interrogated by using SMD in various environments, such as on the surface [22,23] and in liquids [24,25]. The entrapment of enzyme molecules using nanoporous membranes as a solid support holds great promise as a single-molecule analytical technique and as a biophysical model system [26,27]. Artificial membranes including porous silica [28], polymers [29,30] and alumina [31] are known to be thermally and mechanically stable, non-toxic, and highly resistant against microbes and organic solvents [32] compared to their biological counterparts. Such nano-size membranes in the form of a uniform array have the potential to be used for the separation of molecules according to their size [33,34] as well as for enzymatic catalysis [35,36]. Although many studies of enzymes have been carried out using solid-state nanopores, until now they have been limited to the immobilization of the enzyme or the deposition of the desired reagents within the pores.

Herein, we investigate the kinetic of the direct enzymatic digestion of entrapped single-DNA molecules by λ-exonuclease using a nanoporous alumina membrane, prepared *via* the electrochemical modification (anodization) of high purity alumina. One major difference to previous studies [37,38] is that the trapping of the single-DNA molecule inside the nanopore does not require an optical force or an electric field. Unlike surface combing, entrapment also means that a substantial part, if not all, of the DNA strand remain mobile and fully exposed to the reaction buffer [33]. Single-DNA molecules diffuse and randomly reside inside the pores at different depths. The location of the molecule, whether it is caught inside the pore or stays outside the pore, has a potent influence on the digestion rate due to the different local environments. Therefore, the exploration of enzyme digestion of single-DNA molecules using nanopores opens the way for probing the effect of the 3D environment on the digestion rates, including various steric, hydrophobic and electrostatic interactions.

2. Materials and methods

2.1. Reagents and materials

An alumina membrane filter (Whatman International Ltd., Maidstone, UK; 13 mm diameter, 60 μm thick, pore

* Corresponding author. Tel.: +82 31 201 3349; fax: +82 31 202 7337.
** Corresponding author. Tel.: +1 515 294 0105; fax: +1 515 294 0105.
E-mail addresses: shkang@khu.ac.kr (S.H. Kang), yeung@ameslab.gov (E.S. Yeung).

0039-9140/$ – see front matter © 2011 Elsevier B.V. All rights reserved.
doi:10.1016/j.talanta.2011.07.058

diameter = 200 nm, porosity = 75%) [39] was used to provide inorganic pores that tend to be neutral. λ-DNA (M_w = 48 502 bp) and circular-ΦX174 RF DNA (M_w = 5386 bp) were obtained from Promega (Madison, WI). The circular-ΦX174 RF DNA molecules were cleaved to produce linear-ΦX174 RF DNA molecules using a one-cut restriction enzyme (RE) according to the digestion conditions recommended by the Restriction Enzyme Usage Information of Promega. 0.1% poly-*l*-lysine (PLL, M_w = 150 000–300 000) solution and cetyltrimethylammonium bromide (CTAB) were supplied by Sigma–Aldrich (St. Louis, MO). λ-Exonuclease enzyme (M_w = 28 kDa; pK_a = 5.29) was obtained from New England BioLabs (Ipswich, MA).

2.2. Preparation of samples

The λ-exonuclease enzyme (0.2 μg/mL) was diluted with a 1× reaction buffer (pH 9.4, 2.5 mM $MgCl_2$, 67 mM glycine–KOH, 50 μg/mL BSA). The DNA sample was labeled with an intercalator, YOYO-1 (Molecular Probes, Eugene, OR) at a molar ratio of one dye molecule per 50 base pairs in 10 mM Gly–Gly buffer solution (pH 8.2) and then diluted to 1 pM in 25 mM CHES buffer (pH 10.5) for single-molecule imaging. Prior to their use, all buffer solutions were filtered through a 0.2-μm membrane filter.

2.3. Cationic-modification of substrate

To facilitate the entrapment of the biomolecules into the alumina pores, a glass slide was modified by immersing it in 2.0 mM cationic-CTAB surfactant at a concentration greater than the critical micellar concentration (CMC) of 0.9–1.1 mM [40] at 25 °C for 1 h. The poly-*l*-lysine (PLL)-coated glass was produced by immersing a glass slide into a 0.1% PLL solution at 25 °C for 1 h.

2.4. Entrapment and digestion of single-DNA molecule

Alumina membrane filters with a neutral charge and hydrophilic in nature (contact angle = 14.4°) were employed to facilitate their sticking to the surface of the bare- and cationic-modified glasses. The nanoporous wells were formed by attaching the membrane filters to the bare- or cationic-modified glass slide. An 8 μL volume of 1× exonuclease reaction buffer solution (pH 9.4) was dropped at the center of the membrane filter to achieve perfect wetting. Subsequently, 4 μL of 1 pM DNA was dropped onto the same area. The individual DNA molecules placed between the alumina sheet and the cover slip randomly approached (i.e., due to Brownian movement) or were sometimes entrapped on the surface of the alumina membrane (Fig. 1A). The cover slip was matched with an immersion oil (Immersol™ 518F, Zeiss, n = 1.518) for the observation of the epifluorescence image. After confirming that one end of the single-DNA molecule is still mobile while the other end is entrapped inside the pore (Electronic Supplementary Information, M1), 0.2 μg/mL enzyme in 1× reaction buffer solution was injected onto the membrane filter from the edge by using capillary force. The digestion rates of the individual molecules by λ-exonuclease were calculated from the decrease in the relative fluorescence intensity of the entrapped DNA recorded at 37 °C by using an epifluorescence microscope (Fig. 1A).

2.5. Single-molecule measurements by epifluorescence microscopy

The epifluorescence experiments were accomplished using a Zeiss Axioskop50 upright microscope (Zeiss, Germany) coupled with a Pentamax 512-EFT/1EIA ICCD camera (Princeton Instruments, Princeton, NJ). Light from a Hg lamp (power 40 W; AttoArc™ Instrumental, Rockville, MD) was used as the excitation source. A filter cube composed of an excitation filter (460–500 nm), a 50-nm wide bandpass filter centered at 535 nm and a dichroic beam splitter (DM505) was used for the detection of the DNA labeled with YOYO-1. Another filter cube composed of an excitation filter (540 nm), a 40-nm wide band-pass filter centered at 585 nm and a dichroic beam splitter (DM575) was used for the detection of the enzyme labeled with Alexa Fluor® 532. A dichroic beam splitter was used to reflect the light into the back aperture of the objective lens (EC Plan-NEOFLUAR, Zeiss 100×/1.3 N.A., W.D. = 0.2 mm, oil type). To reduce photobleaching, the beam was transmitted through an Uniblitz mechanical shutter (model LS2Z2, Vincent Associates, Rochester, NY) with a VMM-D1 shutter driver (model T132, Vincent Associates). The sampling frequency was 5 Hz with the shutter driver set to an exposure of 10 ms and a delay of 190 ms. The temperature was maintained at 37 °C by using a temperature controller (FRYER, A-50). The single-molecule fluorescence images were collected using WinView/32™ (Version 2.5.14.1, Princeton Instruments) and analyzed using Image J 1.41n software.

3. Results and discussion

3.1. Environment of nanoporous alumina membranes

Fig. 1B shows the scanning electron microscope (Amray 1845FE-SEM, USA) image of the regularly arrayed and uniform (diameter = 200 nm) cylindrical tubes of the alumina membranes used as the containers. The membrane charge is one of the most important factors affecting the interaction between the molecules and the membrane. Furthermore, it is well known that the charge of alumina depends on the pH, due to its being an amphoteric material with an isoelectric point (pI) [41]. Ma and Yeung showed that alumina membranes have a low affinity for DNA at pH 9.0–10 [33]. In this study, we monitored the digestion of DNA by the enzyme in 1× exonuclease reaction buffer (pH 9.4) to minimize any electrostatic effect between the nanoporous membrane and the DNA molecules.

3.2. Surfaces with neutral and cationic charges

To increase the interaction between the DNA molecules and the surface, the bare glass was modified by immersing it in CTAB solution as a cationic-surfactant or in PLL solution. The DNA molecules (pH 10.5) moved randomly on the bare glass slide (Fig. 2A, arrow), but was adsorbed in the linear form on the two cationic-modified glass substrates due to electrostatic force, as shown in Fig. 2B and C, respectively. However, the environment created by putting the nanoporous alumina membrane on the cationic-modified glass substrate did not allow the molecules to be trapped inside the nanopore (Fig. 2D and E, arrows). Therefore, as a substrate, we used a bare glass slide without any chemical modification. In this way the electrostatic force between the slide and the DNA inside the alumina pore (60 μm in depth) was relatively weak to allow entrapment.

3.3. Steric effect of alumina nanoporous membrane

Most of the DNA molecules moved randomly on the alumina membrane surface under bulk flow. By comparing λ-DNA molecules with a different size DNA (5.4 kb) molecules in both the neutral and cationic modified glass environments, we found that the electrostatic force on the DNA molecules was low, regardless of their size, under the same conditions as those indicated in Fig. 2. Although some 5.4 kb-DNA (1.84 μm) molecules were adsorbed on the cationic-modified glass slide (Fig. 3B and C), most of the 5.4 kb-DNA molecules moved randomly on the alumina surface

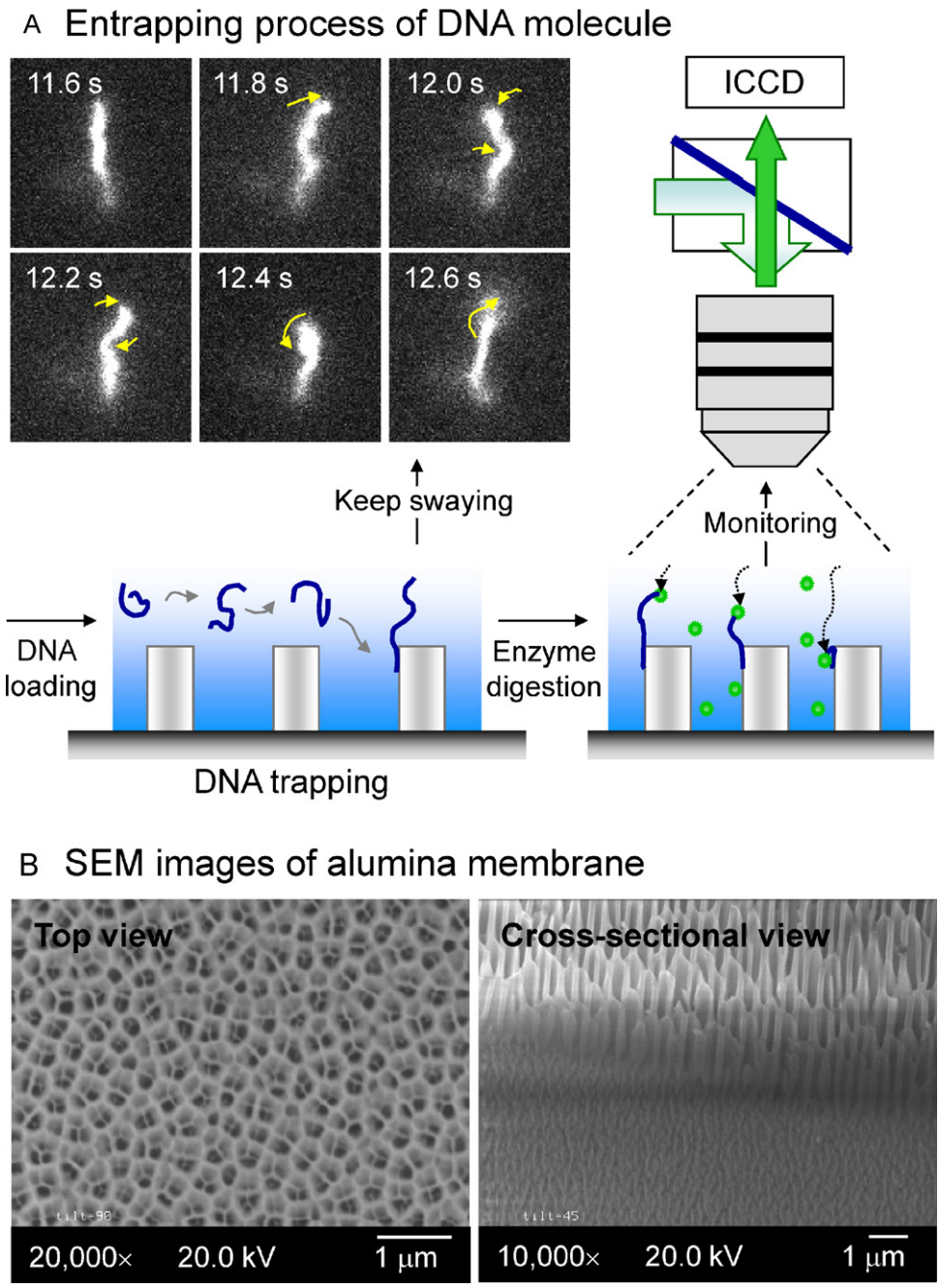

Fig. 1. (A) Entrapment of single-DNA molecules at an alumina nanopore and enzymatic digestion of the entrapped DNA as observed by epifluorescence microscopy. (B) SEM images of the top view and cross-sectional view of the alumina membrane.

with bulk flow (Fig. 3D and E) and thus did not behave differently from λ-DNA molecules. This result indicates that alumina has a low affinity for DNA in this environment. The electrostatic force on the DNA molecules due to the microscope slide is low, regardless of their size, due to the thickness of the alumina membrane of about 60 μm. We also found that DNA fragments with a length >6.6 μm (~20 kb) can become trapped in the 200 nm pores for extended periods. When the DNA length was much shorter than 6.6 μm (e.g., 5.4 kb-DNA), the fragments could not be trapped in the 200 nm alumina pore, i.e., they can diffuse back out even when they move inside the pores. So, the immobilization of DNA molecules was primarily due to entrapment within the nanopores according to the geometry of the alumina pores and not due to adsorption.

3.4. Digestion of single-DNA molecule by λ-exonuclease at different locations from the alumina pore

After loading the DNA samples between the alumina pore and the cover slip, most of the DNA molecules moved randomly on the alumina surface, but some of them were entrapped. The free end of the DNA molecule remains mobile while the other end was entrapped in the neutral environment and can be digested with the addition of λ-exonuclease enzyme. Fig. 4 shows the progression of the two types of single-DNA molecules according to the location of the DNA fragment during digestion. For most of the DNA molecules (77%), a small length of the molecule remained immobilized and continued to sway after the enzyme reaction was terminated (Fig. 4A inset). This indicates that digestion occurred

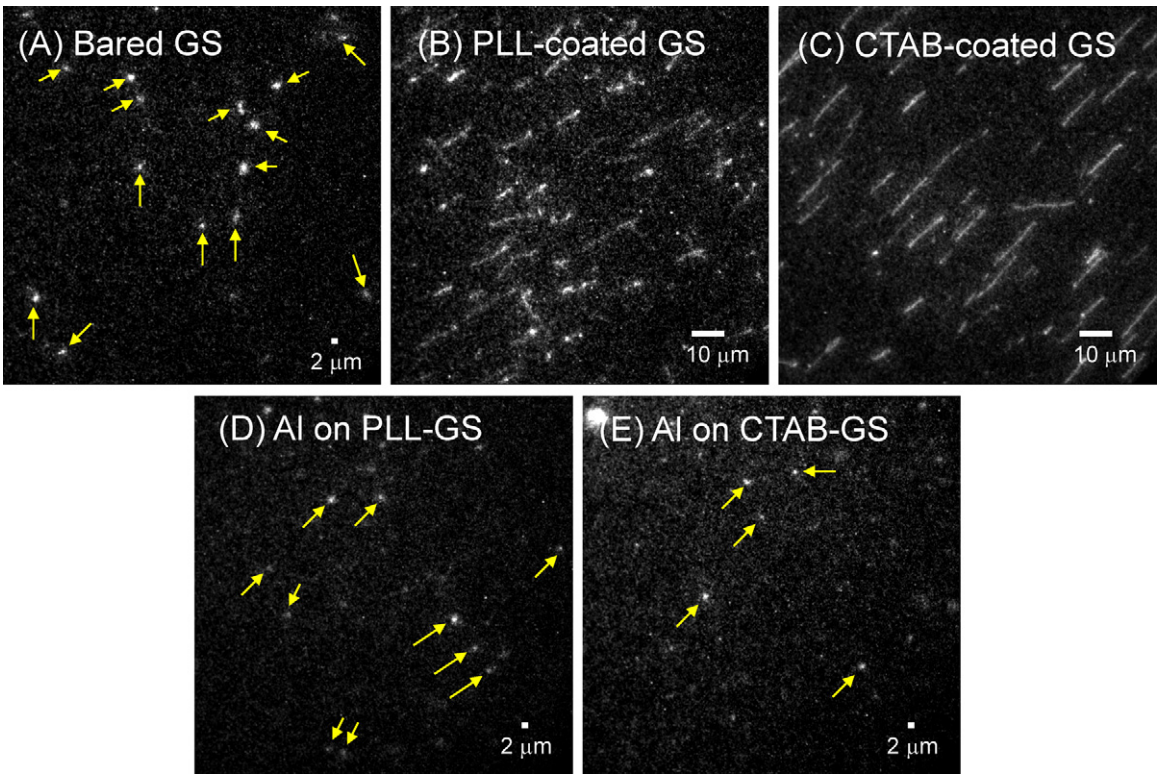

Fig. 2. Typical imaging of interaction patterns of λ-DNA molecules on bare- and cationic-modified substrates. Microscope, Zeiss Axioskop 50 upright microscope; exposure time, 10 ms (5 Hz); sample, λ-DNA (1 pM); dye:bp = 1:50. *GS, glass slide; arrows, mobile DNA molecules.

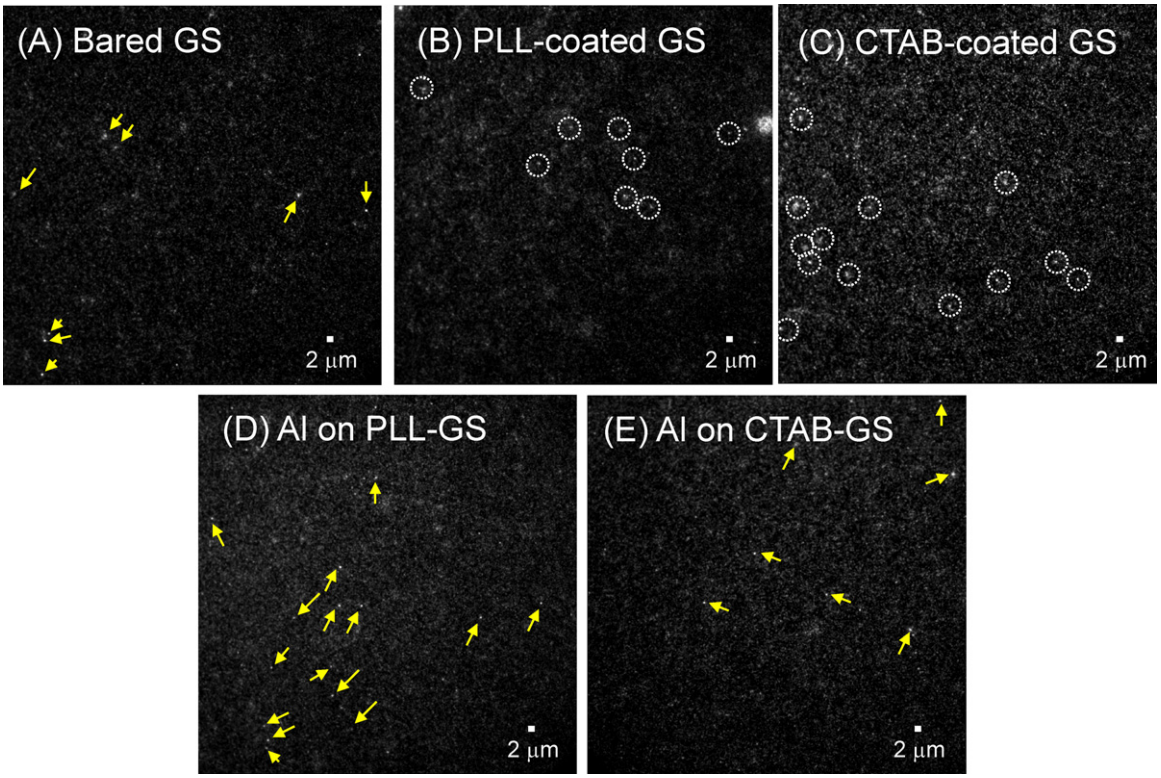

Fig. 3. Typical images of interaction patterns of 5.4 kb-DNA molecules on bare- and cationic-modified substrates. Other conditions were the same as those in Fig. 2. *GS, glass slide; arrows, moving DNA molecules; circles, adsorbed DNA molecules.

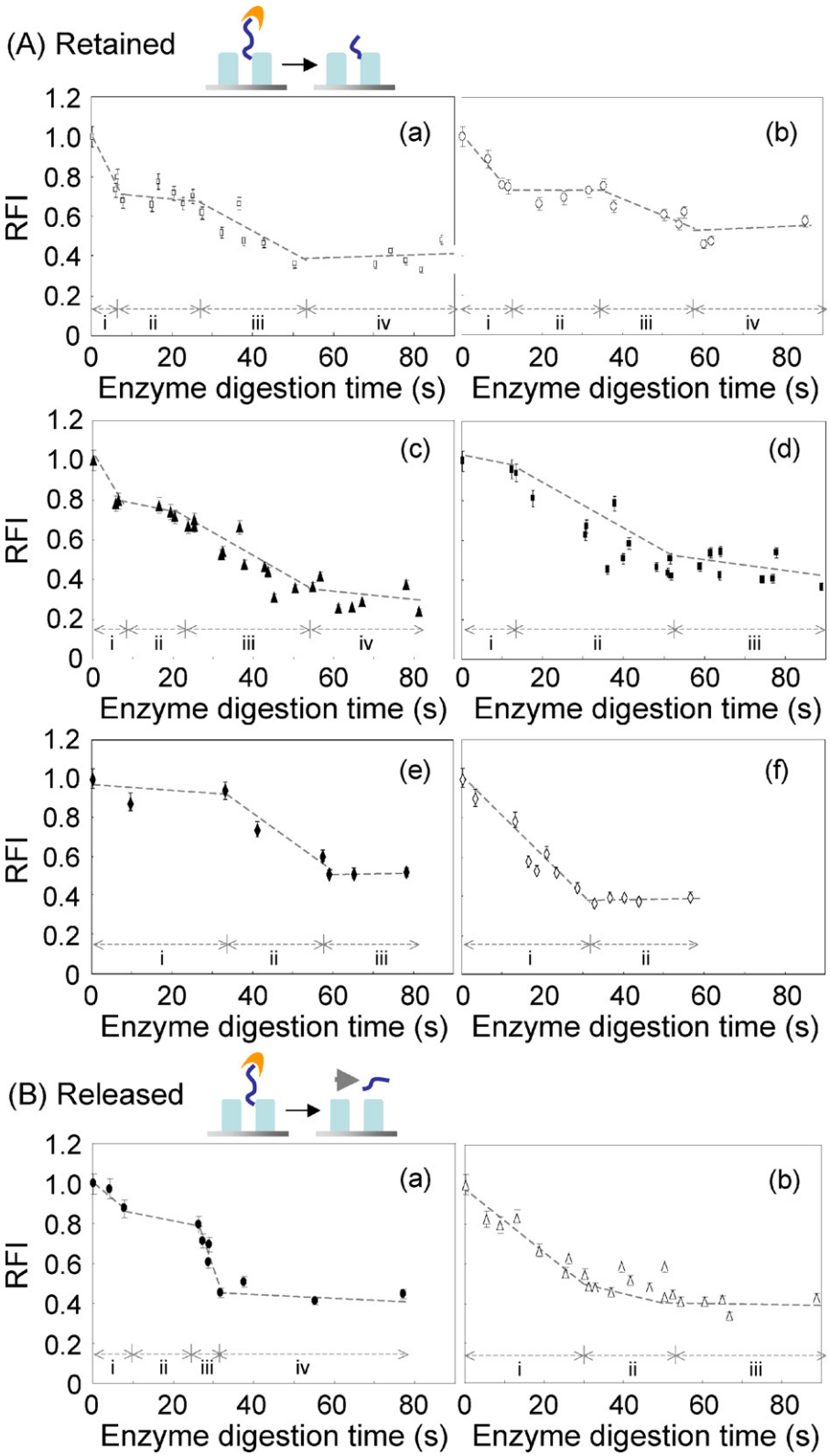

Fig. 4. Real-time digestion of individual λ-DNA molecules by λ-exonuclease as shown by the decrease in the fluorescence intensity: (A) with residual DNA fragment, (B) with wandering DNA fragment after the completion of the digestion reaction. The RFI values were calculated from the fluorescence intensities after subtracting the background. Enzyme, λ-exonuclease (0.2 μg/mL); substrate, bared glass; membrane, 200 nm alumina; buffer, 25 mM CHES (pH 10.5). The other conditions were the same as those in Fig. 2. The different symbols indicate the different patterns of DNA digestion rates. The *x*-axis labeled-i, ii, iii and iv indicate the different regions of DNA digestion rates, which were made from the transformation points of digestion rates.

Table 1
Enzyme digestion rates[a] of individual entrapped λ-DNA molecules by λ-exonuclease based on the decrease in the relative fluorescence intensity (RFI). λ-DNA molecules were labeled with YOYO-1 (dye:bp = 1:50, mol/mol).

Molecule	Regime			
	i	ii	iii	iv
Trapped [bp/s (m/s)]				
a	1827 ± 344 (0.62 ± 0.12)	140.7 ± 9.5 (0.047 ± 0.003)	542.1 ± 72.4 (0.18 ± 0.02)	42.2 ± 13.0 (0.014 ± 0.004)
b	1143 ± 98 (0.39 ± 0.03)	7.2 ± 1.2 (0.0024 ± 0.0004)	346 ± 34 (0.12 ± 0.01)	70.0 ± 16.6 (0.02 ± 0.01)
c	1734 ± 212 (0.59 ± 0.07)	250.4 ± 45.8 (0.09 ± 0.02)	512.0 ± 6.4 (0.174 ± 0.002)	33.2 ± 15.9 (0.011 ± 0.005)
d	223.4 ± 34.3 (0.076 ± 0.012)	548.3 ± 79.2 (0.19 ± 0.03)	64.8 ± 8.3 (0.022 ± 0.003)	–
e	108.4 ± 25.4 (0.04 ± 0.01)	744.7 ± 93.5 (0.25 ± 0.03)	27.7 ± 3.2 (0.009 ± 0.001)	–
f	875.9 ± 101.8 (0.30 ± 0.03)	2.0 ± 0.3 (0.0007 ± 0.0001)	–	–
Free [bp/s (m/s)]				
a	716.9 ± 1.3 (0.24 ± 0.04)	248.2 ± 60.2 (0.08 ± 0.02)	3072 ± 449 (1.05 ± 0.15)	6.3 ± 2.9 (0.002 ± 0.001)
b	753.5 ± 30.6 (0.25 ± 0.01)	243.1 ± 37.0 (0.08 ± 0.01)	9.7 ± 2.5 (0.003 ± 0.001)	–

[a] Mean ± standard deviation (n = 5).

only outside the pores. Occasionally (23% of the molecules), we observed that the digested fragment of the λ-DNA molecule was released and wandered along the surface at different time points while extending and contracting as a random coil (Fig. 4B inset).

The graphical presentation of the digestion rate of the individual molecules showed more than one slope. Graphs "a–c" in Fig. 4A show 4 distinct sets of digestion rates. The digestion rate within region "i" in Fig. 4A was faster than those in the other regions during the first 12 s. The digestion rate in region "ii" was much slower. Region "iii" showed a fast but different digestion rate compared to region "i". Plots "d and e" for region "i" exhibited steady state digestion with an initial rate smaller than those of the other plots. Plot "f" showed just one transition point with a fast digestion rate during the first ~30 s in region "i". Occasionally, the digested fragments of a λ-DNA molecule were released and carried away from the pore (Fig. 4B). Both plot "f" in Fig. 4A and plot "a" in Fig. 4B showed that the relative fluorescence intensity of the molecule decreased during the initial 30 s. However, region "i" of "a" in Fig. 4B showed a digestion event that resulted in 2.15 μm of the λ-DNA molecule being located outside of the alumina pore. Finally, in region "iii" there showed a rapid increase in the digestion rate.

Most of the DNA molecules did not disappear completely and continued to exhibit a swaying motion after ~55 s ("a–e" in Fig. 4A and "b" in Fig. 4B) or ~32 s ("f" in Fig. 4A and "a" in Fig. 4B). We followed the location of the λ-exonuclease enzyme molecules by imaging Alexa 532 labeled-enzyme. We observed that the enzyme molecules were carried along by the flow on the surface (arrow in Fig. S1) and were entrapped (asterisk in Fig. S1) in the pore. It means they could be presented in both inside and outside of the alumina pores. Therefore, the partial digestion of the individual DNA molecules was not related to the absence or presence of the enzyme (~6.6 μm). Rather, the mechanism is similar to that observed in bulk solution and on the prism surface in our previous report [42], where the enzyme was inactivated or released from the DNA at the position of a nick [43,44], preventing the individual λ-DNA molecules from being completely digested.

It was very difficult to reliably measure the decrease in the length of the DNA caused by the enzyme because of the random swaying and coiling of the DNA molecule. Therefore, the enzymatic digestion rates of the individual molecules were calculated based on the decrease in the relative fluorescence intensity and assuming that each molecule had an estimated initial length of 16.5 μm (Table 1). The stochastic variations in the digestion rates are not surprising. Based on the goodness-of-fit, we can group the observed rates into several categories, as displayed in Table 2. λ-exonuclease is a processive enzyme. It has been shown previously that having low levels of YOYO dye on the DNA do not significantly alter the digestion rate. So, one can assume that rate A corresponds to continuous action by the same enzyme molecule. Indeed, the range of rates represented by A is consistent with earlier reports that the free-solution digestion rate is 1000–3000 bp/s. For type B digestion, the rates are roughly one-half that of type A. In such cases, the DNA strand has already been shortened. However, the location of the enzyme is still far (microns away) from the surface and should not be influenced by that. Besides, electrostatic effects have been shown, *vide infra*, not to be important at the alumina surface. It is therefore likely that the more restricted motion on shortening limits the adequate mixing of the reaction buffer around the enzyme, thereby slowing down the digestion process. The rate was even slower in the type C regime. Because that typically occurred between regimes with higher digestion rates, one can assume that the enzyme was partially separated from the DNA strand. The fact that the rate for type C was not zero suggests that the enzyme was not completely released, and was able to continue to digest the strand in an inefficient on/off manner. Type D digestion was observed when the enzyme was very close to the surface. In addition to restricted motion of the DNA strand, surface effects such as adsorption of the enzyme could come into play. The enzyme finally detached from the DNA strand so no activity was observed in the type E regime.

Table 2
Enzyme digestion rates of individual entrapped λ-DNA molecules by λ-exonuclease based on the decrease in the relative fluorescence intensity (RFI). λ-DNA molecules were labeled with YOYO-1 (dye:bp = 1:50, mol/mol). A, >700 bp/s; B, 550–300 bp/s; C, 300–100 bp/s; D, <100 bp/s; E, negligible rate.

Molecule	Regime			
	i	ii	iii	iv
Trapped				
a	A	C	B	D
b	A	E	B	D
c	A	C	B	D
d	C	B	D	–
e	C	A	D	–
f	A	E	–	–
Free				
a	A	C	A	E
b	A	C	E	–

4. Conclusions

We studied the real-time digestion of entrapped single-DNA molecules by enzyme on a nanoporous alumina membrane using an epifluorescence microscope. The alumina pores with a neutral charge did not adsorb DNA or enzyme molecules. When one end of the DNA molecule was entrapped in the alumina pore, the digestion of the free and swaying end was initiated by the addition of λ-exonuclease enzyme. We calculated the enzyme digestion rates

based on the decrease in the relative fluorescence intensity, and confirmed the location and length of the individual DNA molecules according to the images. The DNA molecules show different digestion rates depending on their locations due to restricted motion and, to a smaller extend, surface adsorption. These results open the way for new enzymatic studies to be conducted using nanopores at the single-molecule level and reveal how the enzymatic digestion of individual DNA molecules would be affected by different local environments.

Acknowledgements

The Ames Laboratory is operated for the U.S. Department of Energy by Iowa State University under Contract No. DE-AC02-07CH11358. This work was supported by the Director of Science, Office of Basic Energy Sciences, Division of Chemical Sciences.

Appendix A. Supplementary data

Supplementary data associated with this article can be found, in the online version, at doi:10.1016/j.talanta.2011.07.058.

References

[1] H. Yokota, K. Saito, T. Yanagida, Phys. Rev. Lett. 80 (1998) 4606.
[2] P. Schwille, F.J. Meyer-Almes, R. Rigler, Biophys. J. 72 (1997) 1878.
[3] T. Ha, I. Rasnik, W. Cheng, H.P. Babcock, G.H. Gauss, T.M. Lohman, S. Chu, Nature 419 (2002) 638.
[4] I. Braslavsky, B. Hebert, E. Kartalov, S.R. Quake, Proc. Natl. Acad. Sci. U.S.A. 100 (2003) 3960.
[5] B. Schuler, E.A. Lipman, W.A. Eaton, Nature 419 (2002) 743.
[6] X. Zhuang, M. Rief, Curr. Opin. Struct. Biol 13 (2003) 88.
[7] N. Baudendistel, G. Müller, W. Waldeck, P. Angel, J. Langowski, Chem. Phys. Chem. 6 (2005) 984.
[8] N. Kaji, M. Tokeshi, Y. Baba, Chem. Rec. 7 (2007) 295.
[9] N. Kaji, M. Tokeshi, Y. Baba, Anal. Sci 23 (2007) 21.
[10] Fister J.C.IIIF S.C., L.M. Jacobson, J.M. Davis, Ramsey, Anal. Chem. 70 (1998) 431.
[11] D.T. Mitchell, S.B. Lee, L. Trofin, N. Li, T.K. Nevanen, H. Soderlund, C.R. Martin, J. Am. Chem. Soc. 124 (2002) 11864.
[12] M. Lakadamyali, M.J. Rust, H.P. Babcock, X. Zhuang, Proc. Natl. Acad. Sci. U.S.A. 100 (2003) 9280.
[13] H. Lu, L. Xun, X.S. Xie, Science 282 (1998) 1877.
[14] L. Edman, Z. Földes-Papp, S. Wennmalm, R. Rigler, Chem. Phys. 247 (1999) 11.
[15] L. Edman, R. Rigler, Proc. Natl. Acad. Sci. U.S.A. 97 (2000) 8266.
[16] Y. Chen, D. Hu, E.R. Vorpagel, H.P. Lu, J. Phys. Chem. B 107 (2003) 7947.
[17] S. Myong, I. Rasnik, C. Joo, T.M. Lohman, T. Ha, Nature 437 (2005) 1321.
[18] Q. Xue, E.S. Yeung, Nature 373 (1995) 681.
[19] D.B. Craig, E.A. Arriaga, J.C.Y. Wong, H. Lu, N.J. Dovichi, J. Am. Chem. Soc. 118 (1996) 5245.
[20] D.B. Craig, E.A. Arriaga, J.C.Y. Wong, H. Lu, N.J. Dovichi, Anal. Chem. 70 (1998) 39A.
[21] R. Polakowski, D.B. Craig, A. Skelley, N.J. Dovichi, J. Am. Chem. Soc. 122 (2000) 4853.
[22] P. Ye, R.-B. Wan, X.-P. Wang, J. Mol. Cat. B Enzyme 61 (2009) 296.
[23] J. Lu, M. Ye, N. Duan, B. Li, Nanoscale Res. Lett. 4 (2009) 1029.
[24] M. Gao, P. Zhang, G. Hong, X. Guan, G. Yan, C. Deng, X. Zhang, J. Chromatogr. A 1216 (2009) 7472.
[25] G.W. Slysz, D.C. Schriemer, Anal. Chem. 77 (2005) 1572.
[26] S.W. Kowalczyk, A.R. Hall, C. Dekker, Nano Lett. 10 (2010) 324.
[27] J. Gao, J. Xu, L.E. Locascio, C.S. Lee, Anal. Chem. 73 (2000) 2648.
[28] J. Lei, J. Fan, C.Z. Yu, L.Y. Zhang, S.Y. Jiang, B. Tu, D.Y. Zhao, Micropor. Mesopor. Mater. 73 (2004) 121.
[29] S. Yu, S.B. Lee, M. Kang, C.R. Martin, Nano Lett. 1 (2001) 495.
[30] Y. Rondelez, G. Tresset, K.V. Tabata, H. Arata, H. Fujita, S. Takeuchi, H. Noji, Nat. Biotechnol. 23 (2005) 361.
[31] Z. Yang, S. Si, C. Zhang, Micropor. Mesopor. Mater. 111 (2008) 359.
[32] W. Tischer, F. Wedekind, Top. Curr. Chem. 200 (1999) 95.
[33] C. Ma, E.S. Yeung, Anal. Chem. 82 (2010) 654.
[34] C. Ma, E.S. Yeung, Anal. Chem. 82 (2010) 478.
[35] A. Yamaguchi, F. Uejo, T. Yoda, T. Uchida, Y. Tanamura, T. Yamashita, N. Teramae, Nat. Mater. 3 (2004) 337.
[36] H. Yang, N. Coombs, A. Kuperman, G.A. Ozin, Nature 379 (1996) 703.
[37] M. van den Hout, I.D. Vilfan, S. Hage, N.H. Dekker, Nano Lett. 10 (2010) 701.
[38] U.F. Keyser, J. van der Does, C. Dekker, N.H. Dekker, Methods Mol. Biol. 544 (2009) 95.
[39] K. Omata, A. Masuda, H. Ishii, H. Suzuki, M. Yamada, Appl. Catal. A Gen. 362 (2009) 14.
[40] M.J. Rosen, Surfactants and Interfacial Phenomena, 3rd edition, Wiley, New York, USA, 2004.
[41] P. Baticle, C. Kiefer, N. Lakhchaf, A. Larbot, O. Leclerc, M. Persin, J. Sarrazin, J. Membr. Sci. 135 (1997) 1.
[42] S. Kang, S. Lee, E.S. Yeung, Analyst 135 (2010) 1759.
[43] S. Matsuura, J. Komatsu, K. Hirano, H. Yasuda, K. Takashima, S. Katsura, A. Mizuno, Nucleic Acids Res. 29 (2001) e79.
[44] D.M. Carter, C.M. Radding, J. Biol. Chem. 246 (1971) 2502.